NeuroImage: Clinical 2 (2013) 440–447

Contents lists available at ScienceDirect

NeuroImage: Clinical

journal homepage: www.elsevier.com/locate/ynicl

Diffuse reduction of white matter connectivity in cerebral palsy with specific vulnerability of long range fiber tracts☆

Zoë A. Englander [a], Carolyn E. Pizoli [a,b], Anastasiya Batrachenko [a], Jessica Sun [b,c], Gordon Worley [b], Mohamad A. Mikati [b], Joanne Kurtzberg [b,c], Allen W. Song [a,*]

[a] Brain Imaging and Analysis Center, Duke University Medical Center, USA
[b] Department of Pediatrics, Duke University Medical Center, USA
[c] The Robertson Cell and Translational Therapy Center, Duke University Medical Center, USA

ARTICLE INFO

Article history:
Received 31 January 2013
Received in revised form 7 March 2013
Accepted 11 March 2013
Available online 22 March 2013

Keywords:
Cerebral palsy
Diffusion tensor imaging
Tractography
Structural connectome
Network disruption

ABSTRACT

Cerebral palsy (CP) is a heterogeneous group of non-progressive motor disorders caused by injury to the developing fetal or infant brain. Although the defining feature of CP is motor impairment, numerous other neurodevelopmental disabilities are associated with CP and contribute greatly to its morbidity. The relationship between brain structure and neurodevelopmental outcomes in CP is complex, and current evidence suggests that motor and developmental outcomes are related to the spatial pattern and extent of brain injury. Given that multiple disabilities are frequently associated with CP, and that there is increasing burden of neurodevelopmental disability with increasing motor severity, global white matter (WM) connectivity was examined in a cohort of 17 children with bilateral CP to test the hypothesis that increased global WM damage will be seen in the group of severely affected (Gross Motor Function Classification Scale (GMFCS) level of IV) as compared to moderately affected (GMFCS of II or III) individuals. Diffusion tensor tractography was performed and the resulting fibers between anatomically defined brain regions were quantified and analyzed in relation to GMFCS levels. Overall, a reduction in total WM connectivity throughout the brain in severe versus moderate CP was observed, including but not limited to regions associated with the sensorimotor system. Our results also show a diffuse and significant reduction in global inter-regional connectivity between severity groups, represented by inter-regional fiber count, throughout the brain. Furthermore, it was also observed that there is a significant difference ($p = 0.02$) in long-range connectivity in patients with severe CP as compared to those with moderate CP, whereas short-range connectivity was similar between groups. This new finding, which has not been previously reported in the CP literature, demonstrates that CP may involve distributed, network-level structural disruptions.

1. Introduction

Cerebral palsy (CP) refers to a group of heterogeneous disorders characterized by the impairment of movement and posture with resultant limitation of activity (Bax et al., 2005). CP remains the most prevalent motor disorder affecting children (Clark and Hankins, 2003), and the common co-morbid deficits in sensation, cognition, communication, and behavior contribute immensely to the burden of the disorder in these patients (Bax et al., 2005; Volpe, 2008). A variety of disturbances in the developing fetal or infant brain may lead to CP with an individual's clinical presentation likely determined by the spatial pattern and extent of gray matter (GM) and white matter (WM) involvement (Folkerth, 2005; Volpe, 2008). Standard clinical neuroimaging identifies gross patterns of injury in 70–90% of cases and provides some useful prognostic information; however, tremendous clinical heterogeneity still exists that limits the utility of this neuroimaging data on an individual basis (Benini et al., 2013; Korzeniewski et al., 2008; Krageloh-Mann and Horber, 2007; Martinez-Biarge et al., 2011; Towsley et al., 2011; Woodward et al., 2006).

Multi-modal and advanced neuroimaging techniques such as diffusion tensor imaging (DTI) show great promise for providing increased sensitivity and specificity of the underlying structure–function relationships related to the neurobehavioral deficits in CP. These advanced neuroimaging techniques are also being explored for the more immediate clinical needs of subgroup classification, prognostication, targeting treatment strategies and treatment monitoring (Benini et al., 2013; Hoon, 2005; Shimony et al., 2008). The latter has become increasingly necessary as more neuroprotective and rehabilitative treatment trials

* Corresponding author at: Brain Imaging and Analysis Center, Duke University Medical Center, Durham, NC 27710, USA. Tel.: +1 919 684 1215; fax: +1 919 681 7033.
E-mail address: allen.song@duke.edu (A.W. Song).

2213-1582/$ – see front matter © 2013 The Authors. Published by Elsevier Inc. All rights reserved.
http://dx.doi.org/10.1016/j.nicl.2013.03.006

are underway. Thus far, neuroimaging data have shown early promise as treatment response biomarkers in neuroprotective therapeutic hypothermia (Porter et al., 2010; Rutherford et al., 2010), stem cell therapies (Lee et al., 2012; Min et al., 2013) and rehabilitative trials within this population (Sutcliffe et al., 2009; Trivedi et al., 2008).

Diffusion weighted imaging techniques, including DTI and diffusion tensor tractography (DTT), are particularly well-suited for the detection of WM microstructural changes (Gerig et al., 2004; Mori and Zhang, 2006) that are thought to contribute heavily to the clinical manifestations of CP. In the last several years, many groups have reported DTI-based ultra-structural WM differences in this population. The majority of studies have predominately focused on regions of the brain associated with putative sensorimotor function and demonstrate variable deficits (Chang et al., 2012; Hoon et al., 2002; Ludeman et al., 2008; Murakami et al., 2008; Rose et al., 2007; Scheck et al., 2012; Trivedi et al., 2010) (for systematic review see Scheck et al. (2012)). For the most part, these studies used similar approaches and typically measure diffusivity and anisotropy within a priori selected WM ROIs related to sensorimotor function. Additional studies utilizing tractography methods were likewise focused on the identification of a priori sensorimotor tracts as ROIs for quantification of diffusivity measurements (Rha et al., 2012; Rose et al., 2011; Thomas et al., 2005; Yoshida et al., 2010).

There are a few DTI studies investigating more global WM deficits in CP, also demonstrating changes in mean diffusivity (MD) and fractional anisotropy (FA) (Lee et al., 2011; Rai et al., 2013). In a tractography study, Nagae et al. found multiple and wide-spread differences in a qualitative assessment of 26 manually defined fiber tracts (Nagae et al., 2007). These studies suggest a more diffuse pattern of white matter injury, and indicate the need for a more comprehensive whole-brain characterization of white matter damage in CP.

Thus far, there have been no DTI studies in CP aimed at quantifying WM connectivity throughout the whole brain using a comprehensive and standardized set of ROIs. Given the neuropathologic evidence of diffuse gross and ultra-structural WM pathology in CP patients (Folkerth, 2005; Hoon, 2005; Volpe, 2003) we investigated the spatial pattern and extent of WM tract differences using whole-brain connectivity analysis in children with CP. Specifically, WM connectivity measures were compared between groups of individuals with severe versus moderate CP (grouped by GMFCS level), in order to test the hypothesis that WM connectivity is affected throughout the brain in proportion to the severity of the disorder.

2. Methods

2.1. Subjects

Participants included children, ages 1 to 5 years, with a clinical diagnosis of bilateral CP and Gross Motor Function Classification System (GMFCS) level of II, III or IV. Participants were part of a randomized, placebo controlled trial of autologous cord blood infusions in children with CP. As part of the study, baseline MRI and functional assessments were performed. The data presented here are the results from baseline imaging findings in a subset of children enrolled in the clinical trial. The subset was restricted to children with predominantly spastic bilateral CP in order to minimize clinical heterogeneity in an effort to identify brain pathologies specific to this discrete population and relatable to functional deficits. Thus, patients were excluded if they had hemiparetic CP (unilateral involvement), predominant dystonic CP, seizure disorder, brain dysmorphogenesis, or known genetic disease. The main structural MRI findings in this cohort are enlarged ventricles accompanied by gross white matter atrophy, and none of these individuals showed evidence of perinatal stroke as the primary etiology. Patients underwent neurological testing of motor control, muscle tone and spasticity, overall flexibility and reflexes, as well as cognitive assessment if able (see below). The physical examinations were performed by two senior clinicians experienced with clinical care of patients with CP. Demographic information is presented in Table 1.

The cohort in this report consists of 17 children (age = 2.4 years ± 1.18). Individuals were divided into two groups based on GMFCS level, a severe group (GMFCS of IV, n = 9, mean age = 1.83 years ± 0.77), and a moderate group (GMFCS of II or III, n = 8, mean age = 3.10 years ± 1.23). The moderate and severe group distinction used here separates the participants according to the precursors of their eventual levels of self-mobility. According to the GMFCS levels, individuals at levels II or III will be able to walk with limitations (possibly with a hand held assistance or mobility device) after age 4, however individuals classified at level IV have more limited self-mobility. GMFCS assessment can be performed on children prior to age 4 and is predictive and reliable of functional abilities throughout development (Palisano et al., 1997, 2007).

Of the 17 children in this cohort, 13 were between 0 and 3 years of age and qualified for neuropsychometric testing with the Bayley Scales of Infant and Toddler Development, Third Edition (BSID-III) (Bayley, 2005). The other 4 children were older than 3 years of age at the time of testing; of these, two were too impaired to be tested,

Table 1
Demographic information of the CP patient cohort.

Subject	GMFCS level	Age (at scan, years)	BSID-III cognitive composite	Abnormal movements	Typography	Gestational age (weeks)
1	IV	1.83	55	Spastic predominant with dystonia	Q	38
2	II	2.5	105	Spastic	D	35
3	IV	1.25	55	Spastic predominant with dystonia	Q	30
4	III	4.42	N/T[b]	Spastic	D	27
5	III	2.08	90	Spastic predominant with dystonia	Q	31
6	IV	1.5	N/T[b]	Spastic predominant with dystonia	Q	31
7	IV	3.75	N/T[a]	Spastic	Q	31
8	II	2.08	100	Spastic	D	41
9	II	4.83	N/T[b]	Spastic	D	38
10	II	2.83	100	Spastic	D	32
11	IV	1.42	90	Spastic	Q	32
12	IV	1.92	55	Spastic predominant with dystonia	Q	32
13	II	4.3	69[c]	Spastic predominant with dystonia	D	38
14	IV	1.17	55	Spastic predominant with dystonia	D	39
15	IV	1.7	N/T[b]	Spastic	Q	40
16	IV	1.95	55	Spastic	Q	30
17	II	1.73	80	Spastic predominant, mixed unspecified	Q	35

[a] Not tested due to language barrier.
[b] Too severely disabled to complete testing.
[c] Tested using WISC-III.

one was not tested due to a language barrier, and one was tested using the WISC-III with a full scale IQ of 69 (Table 1). Of the 13 subjects tested with BSID-III, two children were too severely disabled to complete testing; therefore 11 children in this report (mean age = 1.9 years ± 0.50) were tested with cognitive composite scores shown in Table 1. The GMFCS levels and cognitive scores were correlated using a Kendall-tau rank correlation test and were found to be significantly inversely correlated ($\tau = -0.76$, $p = 0.01$). Therefore, most individuals within the severe CP group (GMFCS = IV) also scored lowest on the cognitive assessment, indicating that most cases impaired motor function was accompanied by impaired cognitive function in our cohort.

All patients were sedated for the MRI scans to limit subject discomfort and motion artifacts. Written informed consent was obtained from the parents of each participant and all study related procedures were approved by the Duke University Medical Center Institutional Review Board.

2.2. Image acquisition

Diffusion weighted images were acquired on a 3 Tesla GE HD scanner (Waukesha, WI) using a 25-direction gradient encoding scheme at $b = 1000$ s/mm^2 with 3 non-diffusion-weighted images to ensure a robust baseline. An echo time (TE) of 70.5 ms and a repetition time (TR) of 12,000 ms were used. Isotropic resolution of 2 mm^3 was achieved using the 96×96 acquisition matrix in a field of view (FOV) of 192×192 mm^2. T1-weighted images were obtained with an inversion-prepared 3D fast spoiled-gradient-recalled (FSPGR) pulse sequence with a TE of 2.5 ms, an inversion time (TI) of 450 ms, TR of 6.5 ms, and flip angle of 12°, at 1 mm^3 isotropic resolution.

2.3. Region of interest parcellation

Region of interest (ROI) parcellation was performed using the JHU-DTI-MNI "Eve" atlas template (Oishi et al., 2009), which was warped into each subject's DTI image space via the Large Deformation Diffeomorphic Metric Mapping (LDDMM) algorithm (Faria et al., 2011; Miller et al., 2005). Each individual patient's warping result was visually inspected to confirm anatomical consistency. ROIs were refined by subtracting WM masks obtained from FAST (FMRIB's Automated Segmentation Tool) to restrict the ROIs to only GM voxels (Zhang et al., 2001). Regions of the atlas associated with the brainstem were combined to create a single WM ROI, which was added back to the ROI set after WM masking was performed. As a result, a total of 63 regions were defined for each individual, 31 GM regions per hemisphere, plus a single region encompassing the brainstem.

2.4. White matter tractography and filtering

Following visual inspection of the data for motion artifacts, diffusion tensors were derived from our 25-direction DTI dataset. Tractography was then performed in the whole brain using a streamline fiber-tracking algorithm (Mori and Zhang, 2006; Mori et al., 1999). Fig. 1 illustrates primary data containing a T2 (baseline b0) image, diffusion weighted image ($b = 1000$), colored FA map, and tractography for a representative subject (GMFCS II, age = 1.73). Inter-regional streamlines (fibers) were defined as those that began and terminated within a pair ROIs, while passing through part of the WM mask. Additionally, a length threshold of 40 mm was applied to the whole brain tractography results in order to classify fibers as either short or long range. To confirm the consistency of our findings, we also used length thresholds ranging from 30 mm to 60 mm to classify fibers. All tractographies and parcellations were performed via a standardized pipeline for each patient without regard for the patients' clinical classification.

2.5. Whole-brain connectome analysis

The whole-brain connectome analysis was carried out to investigate the relationship between regional and inter-regional structural connectedness in the severe versus moderate CP groups, using a pipeline based on the Connectome Mapper Toolkit (http://www.cmtk.org) (Gerhard et al., 2011). The amount of all fibers beginning or ending in a region reflected the *total connectivity* associated with that region, while the amount of fibers between each pair of ROIs was used to indicate *mutual connectivity*. Connections and regions that showed decreased connectivity in the severe group as compared to the moderate group were identified. The probabilities of differences in connectivity measures between groups were obtained using a Kruskal–Wallis non-parametric ANOVA. The directions of the differences were obtained by comparing the means of each group. A matrix of p-values demonstrating significantly different connections was obtained for the group, and corrected for multiple comparisons using false discovery rate correction as implemented by FSL's FDR algorithm (Genovese et al., 2002). This analysis was performed for both the total fibers associated with each ROI (total connectivity) and inter-regional fibers (mutual connectivity). To adjust for WM change across development and volume loss associated with injury, each set of fibers was normalized by total WM volume in each individual. In addition, to examine possible GM ROI volume bias in the connectivity measures, we identified the ROIs that demonstrated significant differences between groups. Finally, the mean FA and MD of the WM in the whole brain were compared between groups. Significance levels of all group differences were obtained using the Kruskal–Wallis test.

3. Results

Whole-brain connectivity analysis revealed several significant findings. Specifically, it was found that in addition to the expected widespread reduction in WM and GM volumes, there was a reduction in total connectivity associated with individual regions as well as inter-regional mutual connectivity reductions between severity groups throughout the brain. It should be noted that, as expected, there was a marked reduction in connectivity involving regions associated with the sensorimotor network, which was detected using the comprehensive and unbiased analysis performed here. Additionally, there was a selective reduction of long-range fibers throughout the brain in severe versus moderate CP that was consistently demonstrated using progressively increasing length thresholds. These findings are discussed in detail as follows.

3.1. Total and mutual connectivities are reduced throughout the brain, including but not limited to putative sensori-motor regions

The amount of fibers associated with each of the 63 anatomical regions were assessed to determine how total regional connectivity was altered in relation to CP severity. Nodes throughout the brain showed a marked reduction in total connectivity in the group of individuals with severe CP as compared to moderate CP. In Fig. 2, the red-yellow spheres represent the regions that showed a significant decrease in total connectivity in severe CP versus moderate CP ($p < 0.05$, corrected for multiple comparisons, with the yellow-red color spectrum indicating the progressing significance levels, and the radii of the nodes proportional to the absolute number of connections on average associated with that region). Regions showing connectivity deficits across groups included regions associated with the putative sensorimotor network, as well as anatomic regions associated with other functionalities. In addition to the bilateral pre- and post-central gyri and brainstem within the sensorimotor network, the most significant total connectivity deficits between groups were seen in the bilateral middle occipital gyri, right inferior and superior occipital gyri, bilateral middle and superior frontal gyri, right lingual gyrus, right inferior temporal gyrus, right

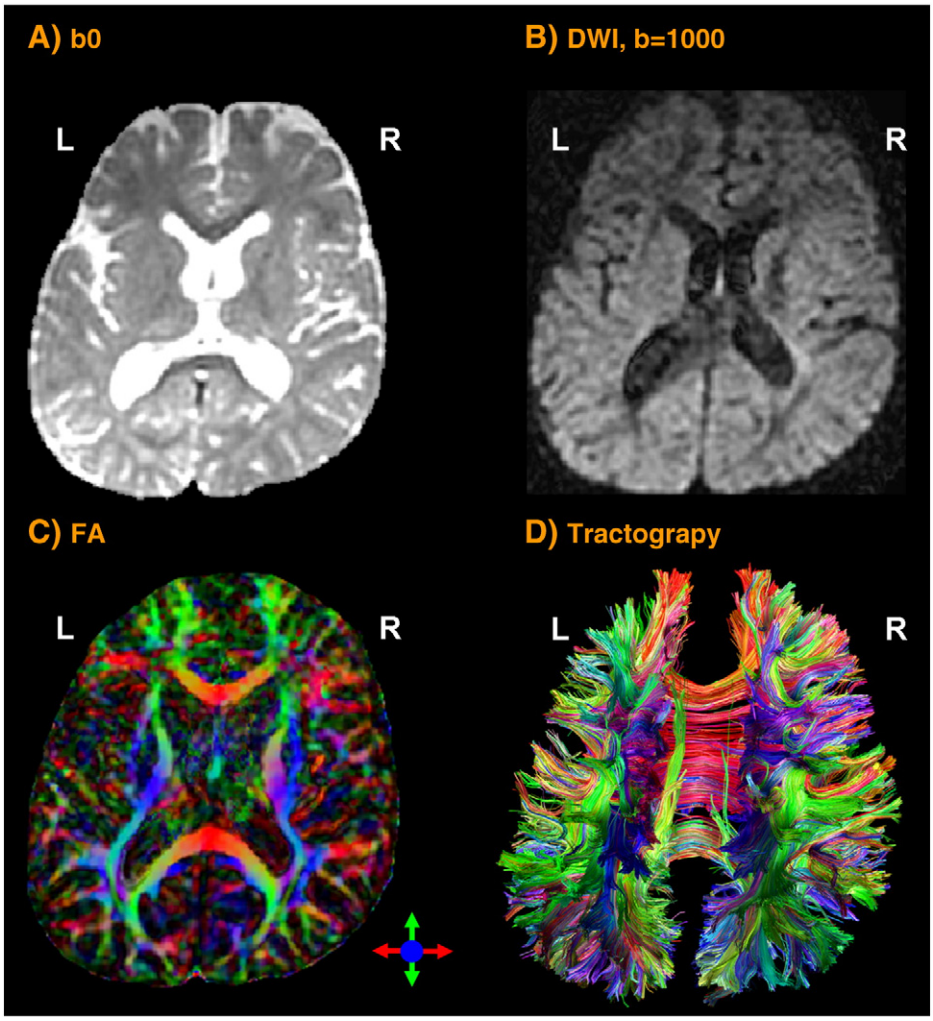

Fig. 1. Primary data images containing (A) T2 (baseline b0), (B) diffusion weighted (b = 1000), (C) colored FA, and (D) tractography from a representative subject (GMFCS II, age = 1.73).

cuneus, left putamen and left superior parietal gyrus. These anatomic regions have been associated with a variety of functional networks, including visual, auditory, and language processing, as well as other higher level cognitive functions such as memory, emotion, and attention. All nodes that demonstrated insignificant changes in total connectivity are shown as gray spheres in Fig. 2.

Mutual connectivities were also analyzed to assess the significance of structural network impairment between CP severity groups. Analogous to the topography of total regional connectivity deficit, our data demonstrated reduced inter-regional fibers throughout the brain with increased CP severity. For all connections between the 63 nodes (ROIs), 75 were significantly reduced in relation to CP severity. Fig. 2 displays the spatial pattern of the significantly reduced mutual connectivity as cool-colored edges ($p < 0.05$, corrected for multiple comparisons). The color gradient of the edges reflects the level of significance, with dark blue indicating the most significant differences in connectivity between severity groups. As expected, significant deficits in mutual connectivity involved regions of the sensorimotor network, including connections between the brainstem and bilateral pre- and post-central gyri, as well as homotopic and interhemispheric edges between the pre- and post-central gyri. Additional significant mutual connectivity reductions in severe versus moderate CP were observed between the right thalamus and right middle occipital gyrus, right superior temporal gyrus and right inferior occipital gyrus, left putamen and superior parietal gyrus, and left putamen and left inferior temporal gyrus, among others. These connections are involved in many functional networks related to perception and cognition, and are representative of the diffuse and global nature of the connectivity deficit between groups seen in this cohort.

Given the diffuse nature of the observed connectivity reductions, we further characterized factors that contributed to this finding. It was observed that there is a significant group difference in whole-brain WM volume between the moderate and severe groups ($p = 0.01$) (Fig. 3A). As WM volume likely changes over the course of brain development, we tested the relationship between WM volume and age using the Kendall-tau rank correlation test, which is appropriate for comparing the continuous variables age and WM volume. As expected, there was a significant relationship ($\tau = -0.4$, $p = 0.02$) between age and total WM volume, justifying the need for using total WM volume as a normalization measure. Subsequently, all connectivity measures were normalized by total WM volume in each subject. As a confirmation of the effectiveness of this control measure, the relationship between age and total fiber volume after correction was investigated using the same correlation test and found to be insignificant ($\tau = 0.28$, $p = 0.18$). In contrast, there was a highly significant group difference in corrected fiber volume ($p = 0.01$), as shown in Fig. 3B, indicating that this group difference is due to CP severity and not age. Additionally, a

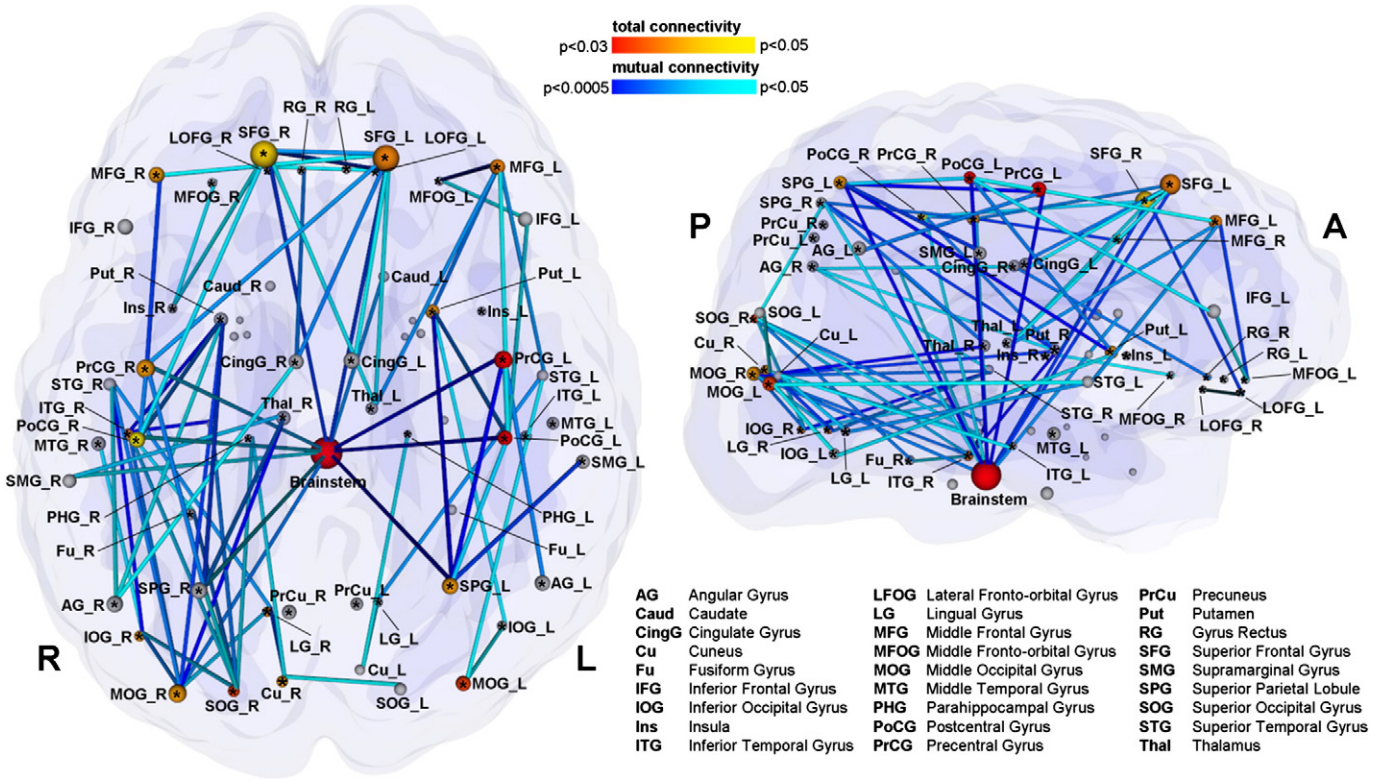

Fig. 2. Inter-regional whole-brain connectivity analysis reveals a diffuse pattern of nodes and edges with significantly reduced connectivity in severe versus moderate CP. A total of 63 nodes (ROIs) are depicted as spheres. The sphere is placed at the center of mass of the ROI, with a radius proportional to the average number of connections across individuals associated with that region. Red-yellow nodes show significantly reduced total connectivity to all other brain regions in severe versus moderate CP ($p < 0.05$, corrected for multiple comparisons). The color gradient of the nodes denotes the significance level of the difference in total connectivity between groups; red nodes indicating the most significantly different between groups. Gray nodes show insignificant differences in total connectivity between groups. Cool-colored edges (connections) between nodes indicate significantly reduced mutual connectivities in the severe CP group as compared to moderate CP group ($p < 0.05$, corrected for multiple comparisons). The color gradient of the edges denotes the significance level of the difference in connectivity between groups; dark blue edges being the most significantly different between groups. Nodes marked with an asterisk (*) indicate ROIs with significant GM volume reduction in severe versus moderate CP. All connectivity measures are normalized by total WM volume in each individual.

decreasing trend was also found in whole-brain WM FA with increasing CP severity (data not shown), as it has already been reported in previous studies (Lee et al., 2011; Rai et al., 2013).

To examine possible GM volume biases, an analysis of ROI volume differences between groups was carried out. Regions that showed a significant ($p < 0.05$, corrected for multiple comparisons) volume reduction between severity groups are denoted with an asterisk in Fig. 2. Although there was some overlap between GM volume and connectivity differences, there was a discrepancy between regions showing reduced GM volume and reduced total and/or mutual connectivity. This indicates that differences in GM volume alone were not sufficient to explain the diffuse structural connectivity changes reported here.

3.2. Specific reduction in long-range connections

Further analysis of our inter-regional connectivity measures, likewise after normalization by total WM volume, demonstrated a length-dependent reduction of mutual connectivities between severity groups. Specifically, a significant difference ($p = 0.02$) in long-range connectivities (≥40 mm in length) was found between severity

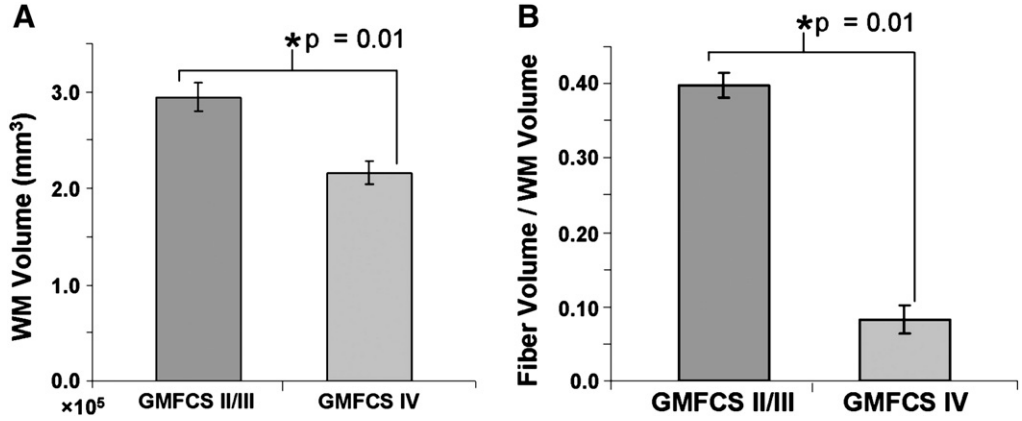

Fig. 3. A: Global WM volume is reduced in severe versus moderate CP ($p = 0.01$); B: Corrected fiber volume (normalized by global WM volume) is reduced in severe vs. moderate CP ($p = 0.01$). Error bars represent standard errors.

groups, with short range connectivities (<40 mm in length) remaining similar between groups, as illustrated in Fig. 4. Additional analyses using different length thresholds were carried out, which continued to show the same pattern of significant group differences. Table 2 summarizes the p-values of the group differences in normalized connectivities of short versus long fibers at systematically progressing length thresholds from 30 mm to 60 mm. These data show that there is a significant reduction in long range connectivities from moderate to severe CP. As expected, the level of significance of this group difference increases with the progressing length threshold, further confirming the long-range connectivity deficit between severity groups.

In a secondary and exploratory analysis, the length dependent reduction in mutual connectivity was examined in relation to cognitive scores. For this analysis, 11 subjects with cognitive composite scores available from the BSID-III were included and grouped into low functioning ($n = 5$, composite scores ≤ 55) and high functioning ($n = 6$, composite scores ≥ 80) groups. The mean long-range mutual connectivities (with respect to the total WM volume) were determined to be 0.04 ± 0.04 in the low functioning group and 0.10 ± 0.05 in the high functioning group. Similar to our previous finding when grouped by motor scores, there appears to be a trend toward the low functioning group having a greater deficit in long-range connectivity than the high functioning group ($p = 0.15$). However, given the noted correlation between the motor and cognitive scores in this cohort, the long range connectivity deficit cannot be yet attributed to either motor or cognitive deficit alone.

4. Discussion

Our results describe differential WM connectivity in severe versus moderate CP in regions associated with the putative sensorimotor network, a finding that is consistent with prior studies (Scheck et al., 2012) and likely relating to the common trait in these patients being motor disturbance. However, the distribution of the observed differences in connectivity was not limited to the sensorimotor network, providing additional support for the role of more widespread WM structural deficits in the pathophysiology of CP.

Indeed, the most salient findings in our whole-brain connectome analysis are the diffuse and length-dependent nature of the WM connectivity deficits in severe versus moderate CP. In particular, we demonstrate a reduction in total and mutual WM connectivities associated with regions throughout the brain between CP severity groups. Notably, the additional length-dependent deficit in connectivity shown here is particularly intriguing given the implications of structural network disruption during development and the variability of motor and cognitive deficits frequently observed in children with CP.

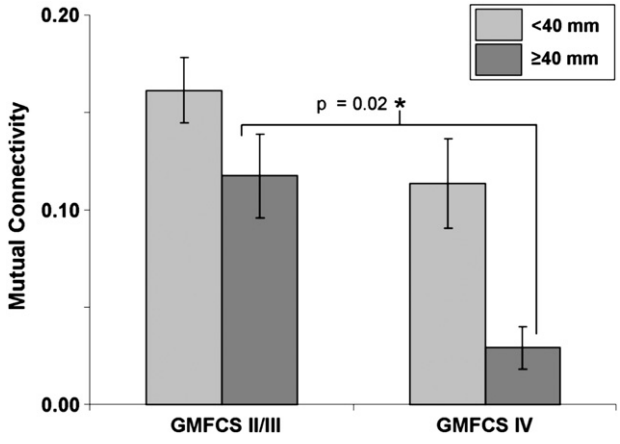

Fig. 4. Long-range mutual connectivity is reduced in severe versus moderate CP. A significant difference ($p = 0.02$) long-range connectivities (≥40 mm) is observed in severe versus moderate CP, while the short-range connectivities (<40 mm in length) remain similar between groups. Connectivity measures were normalized by total WM volume in each individual. Error bars represent standard errors.

Table 2
Short versus long fiber results at different length designations.

Length threshold (mm)	Group difference in normalized mutual connectivity < threshold	Group difference in normalized mutual connectivity ≥ threshold
30	$p = 0.22$	$p = 0.02$*
40	$p = 0.11$	$p = 0.02$*
50	$p = 0.06$	$p = 0.01$*
60	$p = 0.03$*	$p = 0.01$*

* Significant difference ($p < 0.05$).

4.1. Diffuse reduction in total and mutual connectivities

Within the more common perinatally-acquired injuries resulting in CP, different patterns of injury have a preponderance of either WM, diffuse GM, deep gray nuclear or deep gray nuclear/brainstem involvement that relate to the timing and severity of insult that provide etiologically useful distinctions (Hoon, 2005; Krageloh-Mann and Horber, 2007; Volpe, 2008). However, how these multiple and overlapping patterns of injury ultimately manifest symptomatically is not well understood. The variability in symptomatic outcome between and even within any given injury pattern precludes accurate clinical classification, prognostication and treatment targeting. Advances in neuroimaging show promise in providing additional evidence to improve the sensitivity and specificity of linking injury patterns to clinical phenotypes.

To achieve a better understanding of how these injury patterns relate to clinical phenotypes, we used an unbiased, standardized and comprehensive approach to assess WM connectivity, in an effort to explore structural network disruptions throughout the brain in relation to neurodevelopmental outcomes in CP. Our data demonstrate total connectivity deficits involving diffuse anatomic regions (red-yellow nodes, Fig. 2), including but not limited to regions associated with the sensorimotor network. The diffuse nature of the total connectivity deficits observed here is in line with structural neuroimaging data that has identified a wide range of GM and WM abnormalities and varied neuropathology in CP (Folkerth, 2005; Volpe, 2008) and is possibly related to the additional co-morbid deficits seen in this cohort.

Our data also demonstrate diffuse reductions in mutual connectivity in severe versus moderate CP involving regions associated with many different functional networks. While the majority of DTI studies in the CP literature restricted their analysis to a priori selected WM regions or tracts within putative sensorimotor networks, based on the inter-disciplinary and multi-modal evidence of wide-spread WM damage in CP and the varying results in studies of a priori selected regions, whole-brain WM connectivity analysis may be appropriate in the investigation of network deficits in CP. Reduced WM integrity in the corticospinal tract (Murakami et al., 2008) or the thalamocortical projections (Hoon et al., 2002, 2009) has been repeatedly shown, and is similarly demonstrated in our data, along with a more widespread connectivity deficit, using an unbiased and comprehensive whole brain analysis.

On a related note, such global effects in WM properties and connectivity have been demonstrated in the neuroimaging literature of other acquired brain injuries (Gratton et al., 2012; Kraus et al., 2007). As in other acquired brain injuries such as stroke and TBI, connectivity based neuroimaging approaches may be ideally suited to investigate the impaired brain networks in children with CP, in particular because CP is a disorder that originates from early brain injury and is often diffuse in nature.

4.2. Specific reduction in long-range connectivities

The most novel and significant finding in the present study is the specific reduction in long-range WM connections in children with severe versus moderate CP (Fig. 4). This finding was present throughout the brain and not limited to sensorimotor networks (Fig. 2). Our confirmatory analysis using a range of length thresholds from 30 mm to 60 mm also yielded consistent results on this finding (see Table 2). Specifically, here we note that this finding becomes increasingly more significant with the increasing length threshold, further confirming the presence of long-range connectivity reduction in severe versus moderate CP.

It is possible that the selective vulnerability of long range connections is due to the length of tissue vulnerable to multifocal acute ischemic and inflammatory insults, or related to the developmental establishment and maintenance of tracts that are more likely to traverse areas of prior ischemia and inflammation. The most common cause of brain injury resulting in CP is hypoperfusion in the perinatal period leading to selective neuronal and pre-mylenating oligdendroglial cell death with the timing, severity, and duration of ischemia influencing the injury pattern (Folkerth, 2005; Volpe, 2008). The role of the pre-mylenating oligodendrocyte in the pathophysiology of CP is becoming increasingly apparent, and may relate to the reduction in the long range WM connectivity with increasing CP severity demonstrated here.

The length-dependence of the diffuse connectivity deficits seen here suggests possible structural network dysfunction. Because networks involved in processes such as memory, executive function, attention, and even motor activity involve spatially distant brain regions, they rely the integrity of long range connections to function. Thus, our data 1) support the diffuse nature of pathology in CP and 2) suggest that the pattern of long-range vulnerability may result in network level dysfunction. The common co-morbid neurodevelopmental disabilities associated with CP overlap with other pediatric neurodevelopmental disorders that are being increasingly thought of at a network-level of pathology, suggesting a similar network-level of dysfunction in children with CP. In fact, Lee et al. demonstrate complicated changes in the functional connectivity of motor and thalamocortical networks in children with CP. Their cohort also demonstrated large-scale deficits in WM integrity, but the study was not designed to couple the observed structural and functional deficits directly (Lee et al., 2011). Indeed, previous studies have suggested significant correlations between cognitive deficit and brain injury severity in CP (Rai et al., 2013; Schatz et al., 1997).

In our cohort, the most severely affected showed both motor and cognitive deficits and the greatest reduction in long-range connectivity. This would be consistent with the hypothesis that the neurocognitive impairments may be related to a network of connectivity deficits. However, it is not yet possible to attribute either cognitive or motor deficits to decreases in long range connectivity based on this data alone. Nevertheless, our data does suggest that increased diffuse injury and long range connectivity deficit may affect structural and functional networks, and may contribute differentially to neurocognitive disability and motor disability in children with CP, which can be further explored in future analyses.

Additional shortcomings in our study have also been considered. For example, in our analysis we proceeded under the concept that the amount of fibers linking two anatomical regions is representative of WM tract connectivity and that greater tract volume is indicative of connection integrity. Streamline volume does not completely describe the integrity of WM connectivity; however this metric has been used widely in the literature to reflect the presence and strength of structural connections between distant ROIs (Gerig et al., 2004; Yoshida et al., 2010). We also did not include an age-matched healthy control group for this very young age group due to ethics considerations with sedation and technical challenges without sedation. However, to make up for this design constraint, here we have adopted the strategy of examining connectivity that is scaled with disease severity. The analysis presented here is related to functional outcomes in CP, using DTT to define patterns of structural changes within the spectrum of the disorder.

Because CP by definition results from injury or abnormality to the developing brain, the network "dysfunction" may involve long-term network development in addition to acute injury and future studies can be designed to investigate this further. In a study of preterm infants, Smyser et al. reported altered functional network development in several resting state networks, including the sensorimotor network, supporting this point (Smyser et al., 2010). Thus, structural and functional connectome analyses may provide increased sensitivity to relevant pathology and descriptive patterns of network connectivity that relate to disorder classification, prognosis, and treatment targets in children with CP.

5. Conclusions

In summary, our data emphasize the feasibility and suggest the potential importance of including network-based whole brain analyses when studying CP. We found global impairments associated with regions including, but not restricted to, those that are putatively involved with sensori-motor functionality. Additionally, it was demonstrated for the first time, a specific reduction in long-range connections in severe versus moderate CP, which provides potentially provocative insight into the patho-mechanistic disruption of network development that may relate to motor impairment and other neuropsychological comorbidities of CP.

Acknowledgments

The authors acknowledge the support from the NIH (NS 075017 and EB 009483 to AWS) and the Robertson Foundation (to JK). The authors thank Kathryn Gustafson, PhD for the behavioral assessments, Susan Music for the patient scans, Laura Case DPT, and Stephen Raymond for contributions to the statistical analysis, and Chris Petty for technical assistance. The authors also thank the patients and their families for their contributions to the project.

References

Bax, M., Goldstein, M., Rosenbaum, P., Leviton, A., Paneth, N., Dan, B., Jacobsson, B., Damiano, D., Executive Committee for the Definition of Cerebral, P., 2005. Proposed definition and classification of cerebral palsy, April 2005. Developmental Medicine and Child Neurology 47, 571–576.

Bayley, N., 2005. Bayley Scales of Infant and Toddler Development, 3rd edition. Pearson Assessments, San Antonio, TX.

Benini, R., Dagenais, L., Shevell, M.I., 2013. Normal imaging in patients with cerebral palsy: what does it tell us? Journal of Pediatrics 162, 369–374.

Chang, M.C., Jang, S.H., Yoe, S.S., Lee, E., Kim, S., Lee, D.G., Son, S.M., 2012. Diffusion tensor imaging demonstrated radiologic differences between diplegic and quadriplegic cerebral palsy. Neuroscience Letters 512, 53–58.

Clark, S.L., Hankins, G.D., 2003. Temporal and demographic trends in cerebral palsy—fact and fiction. American Journal of Obstetrics and Gynecology 188, 628–633.

Faria, A.V., Hoon, A., Stashinko, E., Li, X., Jiang, H., Mashayekh, A., Akhter, K., Hsu, J., Oishi, K., Zhang, J., Miller, M.I., van Zijl, P.C., Mori, S., 2011. Quantitative analysis of brain pathology based on MRI and brain atlases—applications for cerebral palsy. NeuroImage 54, 1854–1861.

Folkerth, R.D., 2005. Neuropathologic substrate of cerebral palsy. Journal of Child Neurology 20, 940–949.

Genovese, C.R., Lazar, N.A., Nichols, T., 2002. Thresholding of statistical maps in functional neuroimaging using the false discovery rate. NeuroImage 15, 870–878.

Gerhard, S., Daducci, A., Lemkaddem, A., Meuli, R., Thiran, J.P., Hagmann, P., 2011. The connectome viewer toolkit: an open source framework to manage, analyze, and visualize connectomes. Frontiers in Neuroinformatics 5, 3.

Gerig, G., Gouttard, S., Corouge, I., 2004. Analysis of brain white matter via fiber tract modeling. Conference Proceedings: Annual International Conference of the IEEE Engineering in Medicine and Biology Society. IEEE Engineering in Medicine and Biology Society. Conference 6, 4421–4424.

Gratton, C., Nomura, E.M., Perez, F., D'Esposito, M., 2012. Focal brain lesions to critical locations cause widespread disruption of the modular organization of the brain. Journal of Cognitive Neuroscience 24, 1275–1285.

Hoon Jr., A.H., 2005. Neuroimaging in cerebral palsy: patterns of brain dysgenesis and injury. Journal of Child Neurology 20, 936–939.

Hoon Jr., A.H., Lawrie Jr., W.T., Melhem, E.R., Reinhardt, E.M., Van Zijl, P.C., Solaiyappan, M., Jiang, H., Johnston, M.V., Mori, S., 2002. Diffusion tensor imaging of periventricular leukomalacia shows affected sensory cortex white matter pathways. Neurology 59, 752–756.

Hoon Jr., A.H., Stashinko, E.E., Nagae, L.M., Lin, D.D., Keller, J., Bastian, A., Campbell, M.L., Levey, E., Mori, S., Johnston, M.V., 2009. Sensory and motor deficits in children with cerebral palsy born preterm correlate with diffusion tensor imaging abnormalities in thalamocortical pathways. Developmental Medicine and Child Neurology 51, 697–704.

Korzeniewski, S.J., Birbeck, G., DeLano, M.C., Potchen, M.J., Paneth, N., 2008. A systematic review of neuroimaging for cerebral palsy. Journal of Child Neurology 23, 216–227.

Krageloh-Mann, I., Horber, V., 2007. The role of magnetic resonance imaging in elucidating the pathogenesis of cerebral palsy: a systematic review. Developmental Medicine and Child Neurology 49, 144–151.

Kraus, M.F., Susmaras, T., Caughlin, B.P., Walker, C.J., Sweeney, J.A., Little, D.M., 2007. White matter integrity and cognition in chronic traumatic brain injury: a diffusion tensor imaging study. Brain 130, 2508–2519.

Lee, J.D., Park, H.J., Park, E.S., Oh, M.K., Park, B., Rha, D.W., Cho, S.R., Kim, E.Y., Park, J.Y., Kim, C.H., Kim, D.G., Park, C.I., 2011. Motor pathway injury in patients with periventricular leucomalacia and spastic diplegia. Brain 134, 1199–1210.

Lee, Y.H., Choi, K.V., Moon, J.H., Jun, H.J., Kang, H.R., Oh, S.I., Kim, H.S., Um, J.S., Kim, M.J., Choi, Y.Y., Lee, Y.J., Kim, H.J., Lee, J.H., Son, S.M., Choi, S.J., Oh, W., Yang, Y.S., 2012. Safety and feasibility of countering neurological impairment by intravenous administration of autologous cord blood in cerebral palsy. Journal of Translational Medicine 10, 58.

Ludeman, N.A., Berman, J.I., Wu, Y.W., Jeremy, R.J., Kornak, J., Bartha, A.I., Barkovich, A.J., Ferriero, D.M., Henry, R.G., Glenn, O.A., 2008. Diffusion tensor imaging of the pyramidal tracts in infants with motor dysfunction. Neurology 71, 1676–1682.

Martinez-Biarge, M., Diez-Sebastian, J., Kapellou, O., Gindner, D., Allsop, J.M., Rutherford, M.A., Cowan, F.M., 2011. Predicting motor outcome and death in term hypoxic–ischemic encephalopathy. Neurology 76, 2055–2061.

Miller, M.I., Beg, M.F., Ceritoglu, C., Stark, C., 2005. Increasing the power of functional maps of the medial temporal lobe by using large deformation diffeomorphic metric mapping. Proceedings of the National Academy of Sciences of the United States of America 102, 9685–9690.

Min, K., Song, J., Kang, J.Y., Pt, J.K., Ryu, J.S., Kang, M.S., Jang, S., Kim, S.H., Oh, D., Kim, M.K., Soo, K.S., Kim, M., 2013. Umbilical cord blood therapy potentiated with erythropoietin for children with cerebral palsy: a double-blind, randomized, placebo-controlled trial. Stem Cells 31, 581–591.

Mori, S., Zhang, J., 2006. Principles of diffusion tensor imaging and its applications to basic neuroscience research. Neuron 51, 527–539.

Mori, S., Crain, B.J., Chacko, V.P., van Zijl, P.C., 1999. Three-dimensional tracking of axonal projections in the brain by magnetic resonance imaging. Annals of Neurology 45, 265–269.

Murakami, A., Morimoto, M., Yamada, K., Kizu, O., Nishimura, A., Nishimura, T., Sugimoto, T., 2008. Fiber-tracking techniques can predict the degree of neurologic impairment for periventricular leukomalacia. Pediatrics 122, 500–506.

Nagae, L.M., Hoon Jr., A.H., Stashinko, E., Lin, D., Zhang, W., Levey, E., Wakana, S., Jiang, H., Leite, C.C., Lucato, L.T., van Zijl, P.C., Johnston, M.V., Mori, S., 2007. Diffusion tensor imaging in children with periventricular leukomalacia: variability of injuries to white matter tracts. AJNR. American Journal of Neuroradiology 28, 1213–1222.

Oishi, K., Faria, A., Jiang, H., Li, X., Akhter, K., Zhang, J., Hsu, J.T., Miller, M.I., van Zijl, P.C., Albert, M., Lyketsos, C.G., Woods, R., Toga, A.W., Pike, G.B., Rosa-Neto, P., Evans, A., Mazziotta, J., Mori, S., 2009. Atlas-based whole brain white matter analysis using large deformation diffeomorphic metric mapping: application to normal elderly and Alzheimer's disease participants. NeuroImage 46, 486–499.

Palisano, R., Rosenbaum, P., Walter, S., Russel, D., Wood, E., Galuppi, B., 1997. Development and reliability of a system to classify gross motor function in children with cerebral palsy. Developmental Medicine and Child Neurology 39, 214–223.

Palisano, R., Rosenbaum, P., Bartlett, D., Livingston, M., 2007. Gross Motor Function Classification System — Expanded and Revised.

Porter, E.J., Counsell, S.J., Edwards, A.D., Allsop, J., Azzopardi, D., 2010. Tract-based spatial statistics of magnetic resonance images to assess disease and treatment effects in perinatal asphyxial encephalopathy. Pediatric Research 68, 205–209.

Rai, Y., Chaturvedi, S., Paliwal, V.K., Goyal, P., Chourasia, A., Singh Rathore, R.K., Yadav, A., Pandey, C.M., Lalla, R.S., Garg, R.K., Gupta, R.K., 2013. DTI correlates of cognition in term children with spastic diplegic cerebral palsy. European Journal of Paediatric Neurology (Epub ahead of print).

Rha, D.W., Chang, W.H., Kim, J., Sim, E.G., Park, E.S., 2012. Comparing quantitative tractography metrics of motor and sensory pathways in children with periventricular leukomalacia and different levels of gross motor function. Neuroradiology 54, 615–621.

Rose, J., Mirmiran, M., Butler, E.E., Lin, C.Y., Barnes, P.D., Kermoian, R., Stevenson, D.K., 2007. Neonatal microstructural development of the internal capsule on diffusion tensor imaging correlates with severity of gait and motor deficits. Developmental Medicine and Child Neurology 49, 745–750.

Rose, S., Guzzetta, A., Pannek, K., Boyd, R., 2011. MRI structural connectivity, disruption of primary sensorimotor pathways, and hand function in cerebral palsy. Brain Connectivity 1, 309–316.

Rutherford, M., Ramenghi, L.A., Edwards, A.D., Brocklehurst, P., Halliday, H., Levene, M., Strohm, B., Thoresen, M., Whitelaw, A., Azzopardi, D., 2010. Assessment of brain tissue injury after moderate hypothermia in neonates with hypoxic–ischaemic encephalopathy: a nested substudy of a randomised controlled trial. Lancet Neurology 9, 39–45.

Schatz, J., Craft, S., Koby, M., Park, T.S., 1997. Associative learning in children with perinatal brain injury. Journal of the International Neuropsychological Society 3, 521–527.

Scheck, S.M., Boyd, R.N., Rose, S.E., 2012. New insights into the pathology of white matter tracts in cerebral palsy from diffusion magnetic resonance imaging: a systematic review. Developmental Medicine and Child Neurology 54, 684–696.

Shimony, J.S., Lawrence, R., Neil, J.J., Inder, T.E., 2008. Imaging for diagnosis and treatment of cerebral palsy. Clinical Obstetrics and Gynecology 51, 787–799.

Smyser, C.D., Inder, T.E., Shimony, J.S., Hill, J.E., Degnan, A.J., Snyder, A.Z., Neil, J.J., 2010. Longitudinal analysis of neural network development in preterm infants. Cerebral Cortex 20, 2852–2862.

Sutcliffe, T.L., Logan, W.J., Fehlings, D.L., 2009. Pediatric constraint-induced movement therapy is associated with increased contralateral cortical activity on functional magnetic resonance imaging. Journal of Child Neurology 24, 1230–1235.

Thomas, B., Eyssen, M., Peeters, R., Molenaers, G., Van Hecke, P., De Cock, P., Sunaert, S., 2005. Quantitative diffusion tensor imaging in cerebral palsy due to periventricular white matter injury. Brain 128, 2562–2577.

Towsley, K., Shevell, M.I., Dagenais, L., 2011. Population-based study of neuroimaging findings in children with cerebral palsy. European Journal of Paediatric Neurology 15, 29–35.

Trivedi, R., Gupta, R.K., Shah, V., Tripathi, M., Rathore, R.K., Kumar, M., Pandey, C.M., Narayana, P.A., 2008. Treatment-induced plasticity in cerebral palsy: a diffusion tensor imaging study. Pediatric Neurology 39, 341–349.

Trivedi, R., Agarwal, S., Shah, V., Goyel, P., Paliwal, V.K., Rathore, R.K., Gupta, R.K., 2010. Correlation of quantitative sensorimotor tractography with clinical grade of cerebral palsy. Neuroradiology 52, 759–765.

Volpe, J.J., 2003. Cerebral white matter injury of the premature infant-more common than you think. Pediatrics 112, 176–180.

Volpe, J.J., 2008. Neurology of the Newborn, 5th edition. Elsevier, Philadelphia, PA.

Woodward, L.J., Anderson, P.J., Austin, N.C., Howard, K., Inder, T.E., 2006. Neonatal MRI to predict neurodevelopmental outcomes in preterm infants. The New England Journal of Medicine 355, 685–694.

Yoshida, S., Hayakawa, K., Yamamoto, A., Okano, S., Kanda, T., Yamori, Y., Yoshida, N., Hirota, H., 2010. Quantitative diffusion tensor tractography of the motor and sensory tract in children with cerebral palsy. Developmental Medicine and Child Neurology 52, 935–940.

Zhang, Y., Brady, M., Smith, S., 2001. Segmentation of brain MR images through a hidden Markov random field model and the expectation–maximization algorithm. IEEE Transactions on Medical Imaging 20, 45–57.